



# EFFECT OF THE ASPECT RATIO ON THE SEISMIC PERFORMANCE OF POST-TENSIONED CROSS-LAMINATED TIMBER ROCKING WALL SYSTEMS

Gustavo Acuña<sup>1</sup>, J. Daniel Dolan<sup>2</sup>, Irshad Qureshi<sup>3</sup>.

**ABSTRACT:** With the increased interest on the use of Cross-Laminated Timber (CLT) rocking walls as primarily lateral resistance system, some challenges arise, and special considerations might be considered in the design and structural analysis of this type of system. The influence in the dynamic response of the CLT panel aspect ratio is a parameter that has not been thoroughly studied, nor regulated by current codes and standards. The use of narrower panels leads to an amplification of higher-mode effects, due to the lower flexural stiffness of these elements, negatively affecting both the seismic performance and serviceability of this structural system. The objective of this investigation was to determine the variation in the dynamic behavior of a set of mid-rise Post-Tensioned Cross-Laminated Timber rocking wall structures, considering CLT panels with various aspect ratios. Nonlinear time-history analyses, including P- $\Delta$  effects, were performed to predict the seismic behavior. The results clearly showed that the use of wider panels improved the dynamic performance of these type of systems, highlighting reductions in the acceleration and seismic demands, as a consequence of a decrease in the higher-mode amplitudes. Lower aspect ratios also were associated with better displacement, drift ratio, and damage performances.

**KEYWORDS:** Cross-Laminated Timber, Rocking Walls, Aspect Ratio, Higher-Mode Effects, Nonlinear Analysis.

## 1 INTRODUCTION

The use of Post-Tensioned Cross-Laminated Timber (PT CLT) walls as primarily lateral resistant system brings both benefits and challenges. It has been demonstrated that CLT rocking wall systems can potentially withstand major earthquake events, and at the same time represents a viable sustainable construction alternative, which makes it very attractive to the designers. However, one of the major concerns with rocking systems and CLT construction is the important presence of higher modes in their dynamic response, including in low- and mid-rise structures.

Past research (Wiebe and Christopoulos [1], Ceccotti [2], Wiebe et al. [3-4], Qureshi [5], Li [6]) have found and shown the significant contribution of higher modes through testing and numerical simulations. The higher-mode contribution increases the acceleration demand in the entire structure, with a more noticeable effect at the upper stories, producing a whip-action. This increase in the acceleration response also increases the internal forces during seismic excitations, as well as the observable damage at the CLT wall toes. This structural drawback, combined with a drop in the serviceability due to excessive floor accelerations, can potentially reduce the overall feasibility of these type of systems in the mid-rise range. Hence, it is crucial to determine the main factors

that affect the higher-mode amplification in PT CLT rocking wall structures.

One of the factors that can affect the dynamic performance of these rocking systems is the wall aspect ratio. Even the ever-increasing research in rocking systems, the current state-of-the-art has not evaluated its influence on balloon CLT rocking structures as far as the authors can determine. Moreover, the current codes and standards in the United States only provide guidelines for the wall aspect ratio for platform construction in light-frame wood construction. This aspect ratio limitation is provided by the National Design Specification for Wood Construction [7], and naturally, it is tied to the inter-story wall dimensions, rather than its global dimensions.

Therefore, the objective of this investigation was to quantify the difference in the seismic performance of a set of 6-story PT CLT walls with various global aspect ratios. The mean maximum responses of floor accelerations, floor displacements, inter-story drift ratios, shear and moment in the CLT walls, and damaged volume on the CLT wall toes were used as metrics to evaluate the effect of wall aspect ratio. In addition, the higher-mode influence was investigated by analyzing the roof acceleration time-history results.

<sup>1</sup> Gustavo A. Acuña Alegría, Former Doctoral Student, Washington State University, United States, g.acunaalegría@wsu.edu

<sup>2</sup> James Daniel Dolan, Professor Emeritus, Washington State University, United States, jddolan@wsu.edu

<sup>3</sup> Muhammad Irshad Qureshi, Fulbright Scholar, Washington State University, United States, m.qureshi2@wsu.edu

The results presented, herein, are part of the investigation developed by Acuña [8] and are valid only for the structural configurations defined in later sections of this manuscript. These results must be complemented with further research and experimental testing to determine the maximum practical height-to-length ratio for this type of system.

## 2 METHODOLOGY

### 2.1 GENERAL PROCEDURE

The main steps used in this investigation are briefly described in this section. First, the general rocking wall properties were defined, including the number of stories, wall dimensions, seismic weight, and position of the post-tensioned rods. Next, the initial estimates of the seismic demands were computed, following the Equivalent Lateral Force Method (ELF) described by the ASCE 7-16 [9] guidelines.

To determine the number, size, and initial force on the post-tensioned rods, the Cross-Sectional Analysis, developed by Ganey [10] for PT CLT walls, was followed. This method solves the equilibrium equations and stress distributions iteratively to estimate the moment capacity of the post-tensioned rocking wall, given a fixed displacement.

The structures were then evaluated through nonlinear time-history analysis using SAP2000 [11], considering P- $\Delta$  effects. Each individual structure was subjected to forty-four far field traces, scaled to Design Basis Earthquake level, according to ASCE 7-16 [9] procedures.

To determine the frequency content of the roof acceleration time-history responses, Fourier analysis was used with the time trace of the roof response from the program. This approach allowed the amplitude, and therefore the influence, of each mode detected on the acceleration response to be calculated. The Discrete Fourier Transform (DFT) and the Amplitude Spectrum were computed using the MATLAB [12] Function “fft”, corresponding to the “Fast Fourier Transform” algorithm.

### 2.2 MODEL CHARACTERIZATION

The CLT rocking walls were modeled with a simplified 2D model, consisting of a linear elastic frame element to represent the wall panel, and two nonlinear rotational springs at the base of each rocking wall to characterize the rocking behavior. This is a computationally efficient and accurate method of modeling CLT rocking systems, developed by Wilson [13], and it is shown in Figure 1. The modeling technique was further validated against the shake table test results carried out by Pei et al. [14] in a full-scale 2-story post-tensioned CLT rocking wall building. Additional details about the model validation can be found on Acuña [8] and Wilson [13].

U-Shaped Flexural plates (UFPs) were utilized to couple adjacent CLT wall panels and to connect the outer CLT panels to the bounding columns. A rigid foundation was assumed for all the cases. A representation of a 3-panel wall model is illustrated in Figure 2.

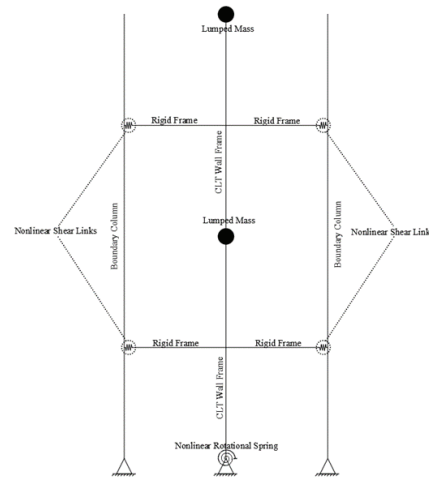


Figure 1: Simplified CLT rocking wall model

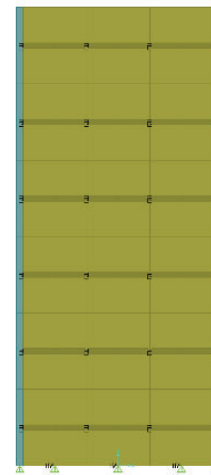


Figure 2: Coupled wall model

### 2.3 SELECTION AND SCALING OF GROUND MOTIONS

Twenty-two far-field acceleration record pairs from the PEER database [15], typically used for FEMA P-695 [16] analyses, were selected for numerical evaluation. Scaling of the traces was carried out following the Amplitude Scaling process, according to ASCE 7-16 [9]; where one single scale factor is used for all the acceleration traces to match the average maximum direction spectrum (RotD100) with the target spectrum at the target period.

The target spectrum was defined assuming the buildings to be in Downtown Seattle, WA (47.622, -122.337). Site Class C and Importance Factor II were assumed for the building, according to ASCE 7-16 [9]. The Modified Response Factor (R-factor) was selected as 6, based on the observations presented by Pei et al. [17], Ganey [10], and Wilson [13]. The design moment demand for all of the structures was 3,192 kN-m. The target spectrum, the mean RotD100 spectrum, and the individual RotD100 spectra for the 22 ground motions are shown in Figure 3.

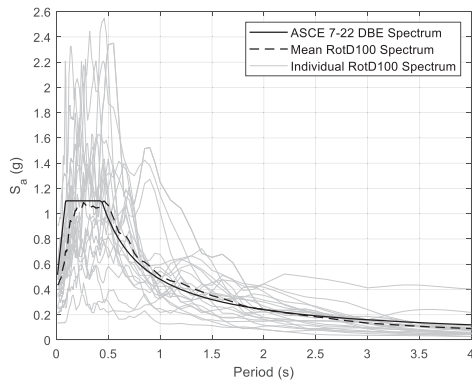


Figure 3: ASCE 7-22, mean RotD100, and individual RotD100 acceleration spectra

### 3 CASE STUDY

#### 3.1 MATERIAL PROPERTIES

##### 3.1.1 Cross-laminated timber

E1M5 rated panels, according to the Structurlam [18] specification, were selected for the CLT rocking walls. The properties of a 9-ply CLT panel were derived from crushing and shear tests performed in a 5-ply CLT panel by OSU and PSU [19]. The adjusted properties for a 9-ply panel were: 7,037 MPa for the modulus of elasticity in the longitudinal direction, 4,520 MPa for the modulus of elasticity in the transverse direction, 552 MPa for the shear modulus, 18.2 MPa for the yield stress, 0.0026 mm/mm for the yield strain, and 0.0082 mm/mm for the crushing strain. The Poisson's ratio was assumed as 0.3 in all directions. The post-yield behavior of the wood crushing was assumed as elastic-perfectly plastic.

##### 3.1.2 Post-tensioned rods

Fully threaded, high-strength steel rods were selected for the PT rods, with denomination ATS-HSRX, according to Simpson Strong-Tie [20]. ATS-HSRX rods use ASTM F1554 Gr.105 steel for diameters equal or greater than 28.58 mm; with modulus of elasticity of 200,000 MPa, yield strength of 724 MPa, and tensile strength of 862 MPa.

##### 3.1.3 U-shaped flexural plates

ASTM A572 Gr.42 steel plates were selected for the UFPs. The elastic modulus was 200,000 MPa, and the yield stress was 290 MPa.

#### 3.2 SPECIMEN DESIGN

Four CLT panel lengths were selected for the numerical evaluation. These panel lengths were chosen to contain the practical range of the CLT panel manufacturing (up to 3.05 m), while an additional length (4.57 m) was included in the analyses for numerical purposes (it is understood that field connecting multiple CLT panels to construct the walls longer than can be manufactured is currently problematic, but for this analysis the connectivity to construct a continuous 4.57 m panel was assumed to be perfect).

For comparison reasons, a target wall length of 9.14 m was defined, and the required number of panels to cover the target length was calculated. These wall segments were connected by using UFPs. The panel length, aspect ratio, and the required number of segments are shown in Table 1.

The number of stories, inter-story height, wall thickness, story weight, roof weight, and position of the post-tensioned rods were held constant throughout all the cases, assuming 6 stories, 3.66 m, 31.43 cm, 333.6 kN, 166.8 kN, and wall centerline respectively. The UFP's size was also held constant; the bend diameter, width, and thickness were set to 15.24 cm, 6.35 cm, and 0.953 cm, respectively.

Table 1: Wall Length and Aspect Ratio

#ID	Wall Panel Length (m)	Aspect Ratio (H:L)	# Segments
1	1.52	14.4 : 1	6
2	2.29	9.6 : 1	4
3	3.05	7.2 : 1	3
4	4.57	4.8 : 1	2

To conduct the performance comparison, the rocking wall structures were designed to provide a similar moment capacity at 2.0% drift ratio. The required PT size, number, and initial force were determined using the Cross-Sectional Analysis. The PT properties are summarized in Table 2, and the moment-drift ratio relationship for the wall specimens are shown in Figure 3.

Table 2: Post-tensioning properties

#ID	$\phi_{PT}$ (mm)	#PT Rods	Segment Initial PT Force (kN)	Specimen Capacity (kN-m)
6-5	28.58	4	667	3,452
6-7.5	28.58	4	489	3,553
6-10	28.58	4	311	3,557
6-15	34.93	2	111	3,510

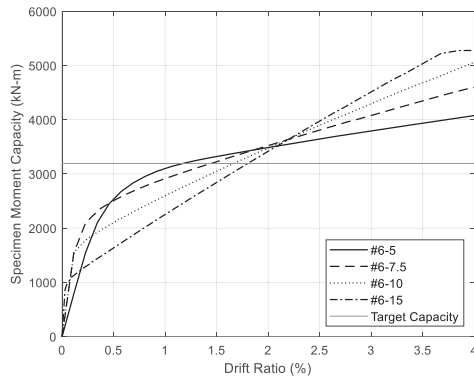


Figure 4: Specimen capacities and target capacity

## 4 RESULTS

The main results from the nonlinear time-history analyses are presented in this section. These results include acceleration, displacement, inter-story drift, shear force, and moment envelopes, modal amplitudes, and damage on CLT walls. The relative differences presented in this section were computed considering the results for Specimen #6-5 as baseline.

### 4.1 ACCELERATION RESPONSE

The time-history analysis results showed that the magnitude of the peak floor acceleration is directly related to the wall aspect ratio. The mean maximum profiles, presented in Figure 4, indicate a reduced acceleration response for specimens with lower global panel aspect ratio, essentially in the entire structure. A decrease in the whip-action at the upper stories is also noticeable, indicating less influence of the higher vibration modes.

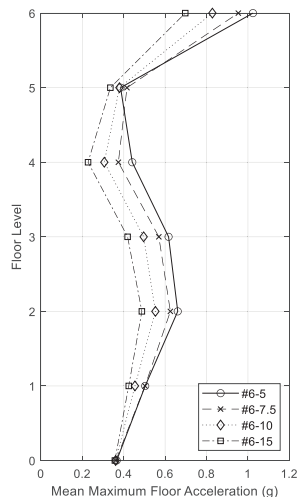


Figure 5: Average peak floor acceleration

It was observed that the largest average peak roof acceleration in Specimen #6-5, had a mean value of 1.02

g, while the smallest peak roof acceleration response was obtained in Specimen #6-15, with a value of 0.70 g. This is a respective difference reduction of 31.4%. The remaining average peak roof accelerations and differences are summarized in Table 3.

Table 3: Average peak roof acceleration

#ID	Average Peak Roof Acceleration (g)	Difference (%)
6-5	1.02	-
6-7.5	0.95	-6.9
6-10	0.83	-18.6
6-15	0.70	-31.4

### 4.2 FREQUENCY ANALYSIS

The 90<sup>th</sup> percentile Fourier amplitude spectra are presented in Figure 5. It is observed that both the first and second mode amplitude increase as the aspect ratio of the wall segment increases, showing the largest amplitudes in Specimen #6-5 and the smallest in Specimen #6-15. A significant shift in the second mode frequency is also exhibited, moving from the 3.5-4.0 Hz range for Specimen #6-5 to the 7.0-7.5 Hz range for Specimen #6-15; this change in the second-mode frequency can potentially reduce the seismic demands by moving the dynamic response out of the plateau region of the design spectrum.

The first and second mode amplitudes for Specimen #6-5 were 0.108 g and 0.145 g, respectively. For comparison, the first and second mode amplitude for Specimen #6-15 were 0.061 g and 0.067 g, respectively. The relative comparison between these two structures yielded an amplitude reduction of 43.5% and 53.8% for first and second mode, respectively. The Fourier amplitudes for the structures considered in this study are shown in Table 6.

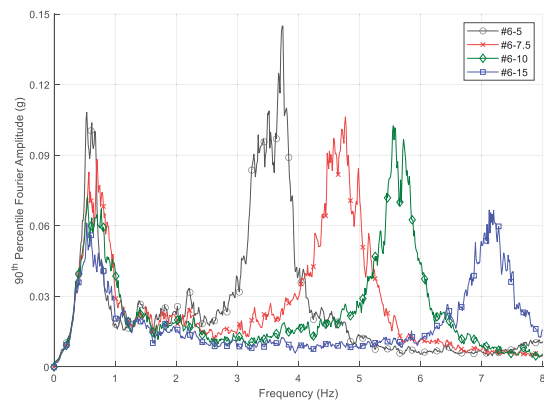


Figure 6: 90<sup>th</sup> percentile Fourier amplitude spectra

**Table 4:** 90<sup>th</sup> percentile Fourier amplitude spectra

#ID\ Mode	Frequency (Hz)		90 <sup>th</sup> Percentile Amplitude (g)		Amplitude Difference (%)	
	1	2	1	2	1	2
	6-5	0.54	3.75	0.108	0.145	-
6-7.5	0.70	4.77	0.088	0.106	-18.5	-26.9
6-10	0.55	5.55	0.072	0.103	-33.3	-29.0
6-15	0.54	7.12	0.061	0.067	-43.5	-53.8

**4.3 DISPLACEMENT RESPONSE**

The average peak floor displacement profiles, shown in Figure 6, increases with the aspect ratio. It can also be observed that the wall aspect ratio impacts the shape of the displacement envelope, indicating a relative change between the different displacement mechanisms.

The largest peak roof displacement was obtained in Specimen #6-5, with an average of 28.7 cm. While, the minimum average peak roof displacement in Specimen #6-15 was averaged 23.1 cm. The displacement difference between these two structures showed a reduction of 19.5%. The remaining peak roof displacements are presented in Table 5.

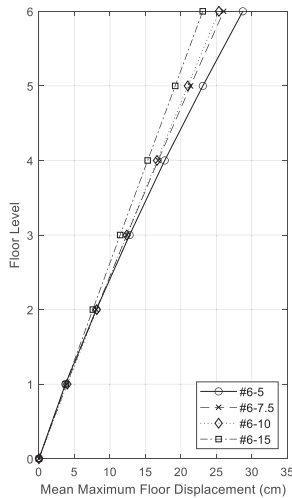


**Figure 7:** Average peak floor displacement

**Table 5:** Average peak roof displacement

#ID	Average Peak Roof Displacement (cm)	Difference (%)
6-5	28.7	-
6-7.5	25.9	-9.7
6-10	25.4	-11.5
6-15	23.1	-19.5

**4.4 INTER-STORY DRIFT RESPONSE**

Similar to the displacement results, the average peak inter-story drift ratio increased as the wall aspect ratio increased. Additionally, it was verified that the rocking behavior governed the displacement response of the structure with the lowest aspect ratio panels, given by its relatively uniform deformation pattern. In contrast, the structure with the highest aspect ratio panels presented a non-uniform drift ratio distribution, with higher drifts in its upper section, indicating an important presence of bending relative to the rocking motion. The average peak inter-story drift profiles are shown in Figure 7.

The analysis results showed that the maximum inter-story drift ratio was produced in Specimen #6-5, with an average of 1.59%. The lowest drift ratio was observed in Specimen #6-15, with an average of 1.07%. Their relative difference resulted in a drift reduction of 32.7%. The rest of the average peak inter-story drift values and differences are presented in Table 6. Note that these peak values are the maximum observations, regardless of where it was produced (i.e., they are not bound to a specific story.)

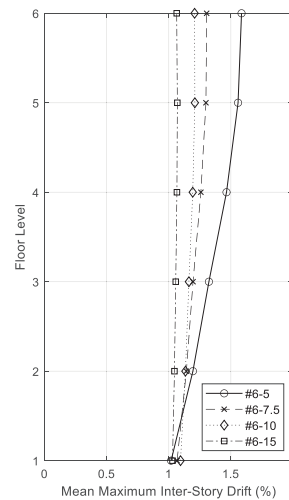


**Figure 8:** Average peak inter-story drift ratio

**Table 6:** Average peak roof displacement

#ID	Average Peak Inter-Story Drift Ratio (%)	Difference (%)
6-5	1.59	-
6-7.5	1.31	-17.6
6-10	1.21	-23.9
6-15	1.07	-32.7

**4.5 SHEAR RESPONSE**

The shear force results, shown in Figure 8, indicate that the use of longer CLT wall segments reduced the seismic forces into the structure. This pattern is observed essentially in the entire structure, and it follows a similar trend as the acceleration envelopes, presented in previous sections. The seismic shear reduction is also a

consequence of the difference on the higher-mode amplitudes.

The largest base shear was observed in Specimen #6-5, with a peak average of 490 kN, while the smallest seismic base shear was on Specimen #6-15 with a maximum average of 358 kN. Their relative difference was a reduction of 26.9%. The rest of the mean maximum base shears are summarized in Table 7.

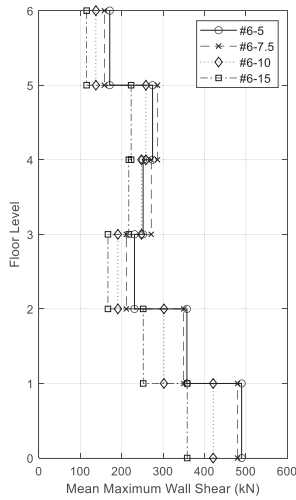


Figure 9: Average peak wall shear

Table 7: Average peak base shear

#ID	Average Peak Base Shear (kN)	Difference (%)
6-5	490	-
6-7.5	480	-2.0
6-10	421	-14.1
6-15	358	-26.9

#### 4.6 MOMENT RESPONSE

The moment results followed a similar pattern compared to the shear force distribution, as shown in Figure 9, presenting the lowest seismic demand in Specimen #6-15. This performance difference was expected, based on the acceleration and modal amplitude results.

The largest average peak base moment was obtained in Specimen #6-5, with a moment of 3,111 kN-m, while the smallest peak moment was observed in Structure #6-15, with a mean maximum base moment of 2,306 kN-m. The improvement in the response was a reduction of 25.9%. The remaining average maximum base moments are summarized in Table 8.

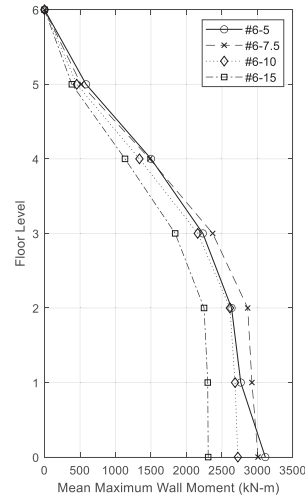


Figure 10: Average peak wall moment

Table 8: Average peak base moment

#ID	Average Peak Base Moment (kN-m)	Difference (%)
6-5	3,111	-
6-7.5	3,008	-3.3
6-10	2,724	-12.4
6-15	2,306	-25.9

#### 4.7 DAMAGED CLT

The damage analysis also continued with the trend observed for the other performance indicators, showing larger damage in the CLT wall toes in structures with higher aspect ratios. This is a direct consequence of the increase of displacements and moment demands for structures with higher wall aspect ratios, as well as for the reduction in their internal lever arm (to achieve a similar moment, there are required higher strains and stresses at the toes, hence more damage is expected).

The maximum average damage was observed on Specimen #6-5, while the minimum damage was obtained on Specimen #6-15. The average damaged volumes for these two configurations were 18,108 cm<sup>3</sup> and 4,097 cm<sup>3</sup>, respectively. The damage difference was a reduction of 77.4%. The remaining CLT damage and their respective percentage differences are summarized in Table 9.

Table 9: Average damaged volume on CLT wall toes

#ID	Average Damaged Volume (cm <sup>3</sup> )	Difference (%)
6-5	18,108	-
6-7.5	11,930	-34.1
6-10	7,833	-56.7
6-15	4,097	-77.4

## 5 CONCLUSIONS

The effect of wall segment aspect ratio on the seismic behavior of CLT rocking walls was determined. The results showed that structures with lower aspect ratios (i.e., wider wall segments) have a better seismic performance than structures with narrower segments, due to a reduction of the higher-mode influence on its dynamic behavior, as demonstrated through the Fourier amplitude spectrum. The mean maximum acceleration, displacement, and drift ratio envelopes reduced as the aspect ratio decreased. The internal forces (story shear and moments) presented identical trends as mentioned before. The aspect ratio of the segments also affected the local performance of the rocking walls, exhibiting less damage on the CLT wall specimens with lower aspect ratios.

Based on the findings of this investigation, it is highly recommended to use longer wall panels rather than a series of slender panels coupled with UFPs. However, further investigations are needed to determine the overall upper bound of the wall aspect ratio for this type of systems, also considering the effect of the total building height. This would be crucial to develop new code regulations for CLT rocking wall systems and potentially fully develop its use in mid-rise construction.

The acceleration results showed the highest response in Specimen #6-5, with an average peak roof acceleration of 1.02 g. The structure with the lowest acceleration response was Specimen #6-15, with an average maximum of 0.70 g. Their relative difference was 31.4%. The shape of the acceleration distributions showed a reduction in the whip-action at the upper stories in structures with lower wall aspect ratio.; this also suggested a reduction on the higher-mode contribution, which was confirmed through the frequency analysis.

The Fourier amplitude spectra showed the difference in the frequency content on the roof acceleration response. It was verified a reduction in both the first- and second-mode amplitude in structures with lower aspect ratios. The relative differences between Specimens #6-5 and #6-15 were reductions of 43.5% and 53.8% for the first and second mode, respectively.

Both the displacement and inter-story drift ratio distributions showed that the increase on the wall aspect ratio increased the influence of bending deformation, relative to the rocking motion. It was also verified that structures with higher aspect ratio presented higher displacements and inter-story drifts. The maximum roof displacement and inter-story drift were found for Structure #6-5, with an average displacement of 28.7 cm and 1.59%, respectively. Structure #6-15 presented the lowest average peak displacement and drift ratios, with mean maximum values of 23.1 cm and 1.07, respectively. Their respective relative differences were 19.5% for displacements, and 32.7% for drift ratios. It was also

verified that the structures presented in this study did not exceed the drift limit of 2.0% specified in ASCE 7-22 for design level earthquakes.

The internal forces presented similar trends, showing a general decrease as the aspect ratio decreases. The maximum base shear and base moment were observed in Specimen #6-5, with values of 490 kN and 3,111 kN-m. The minimum base shear and moment were found on Structure #6-15, with values of 358 kN and 2,306 kN-m. Their relative differences were reductions of 26.9% and 25.9% for shear and moment, respectively.

The damage on the CLT walls increased as the aspect ratio increased. Specimen #6-5 exhibited the largest average damage, with a volume of 18,108 cm<sup>3</sup>, while Specimen #6-15 presented the lowest damage, with an average of 4,097 cm<sup>3</sup>. Their relative difference was 77.4%.

## ACKNOWLEDGEMENT

This work was supported by the scholarship provided by the Chilean Agencia Nacional de Investigación y Desarrollo, ANID (formerly known as Comisión Nacional de Investigación Científica y Tecnológica, CONICYT) PFCHA/Doctorado Becas Chile/2017 - 72180372.

## REFERENCES

- [1] Wiebe, L., and C. Christopoulos: Mitigation of Higher Mode Effects in Base-Rocking Systems by Using Multiple Rocking Sections. *Journal of Earthquake Engineering*, 13 (S1): 83–108, 2009.
- [2] Ceccotti, A., C. Sandhaas, M. Okabe, M. Yasumura, C. Minowa, and N. Kawai.: SOFIE project - 3D shaking table test on a seven-storey full-scale cross-laminated timber building. *Earthquake Engineering and Structural Dynamics*, 42 (13): 2003–2021, 2013.
- [3] Wiebe, L., C. Christopoulos, R. Tremblay, and M. Leclerc: Mechanisms to limit higher mode effects in a controlled rocking steel frame. 1: Concept, modelling, and low-amplitude shake table testing. *Earthquake Engineering and Structural Dynamics*, 42 (7): 1053–1068, 2013.
- [4] Wiebe, L., C. Christopoulos, R. Tremblay, and M. Leclerc: Mechanisms to limit higher mode effects in a controlled rocking steel frame. 2: Large-amplitude shake table testing. *Earthquake Engineering and Structural Dynamics*, 42 (7): 1069–1086, 2013.
- [5] Qureshi, I. M., P. Warnitchai, and T. Mehmood: Investigation of Dynamic Response of Rocking Wall Structures Using Inelastic Modal Decomposition Technique. In *5th ECCOMAS Thematic Conference on Computational Methods in Structural Dynamics and Earthquake Engineering*, 3139–3150. Crete Island, Greece, 2015.
- [6] Li, T., J. W. Berman, and R. Wiebe: Parametric study of seismic performance of structures with multiple rocking joints. *Engineering Structures*, 146: 75–92, 2017.

- [7] American Wood Council. National Design Specification for Wood Construction, Special Design Provisions for Wind & Seismic. ANSI/AWC SDPWS-2018. American Wood Council, Leesburg, VA. 2018.
- [8] Acuña, G.: Effects of Geometric, Damping, and Boundary Parameters on the Dynamic Response of Cross-Laminated Timber Rocking Wall Systems. Doctoral Dissertation. Washington State University, Pullman, WA. 2022.
- [9] American Society for Civil Engineers. Minimum Design Loads and Associated Criteria for Buildings and Other Structures. ASCE/SEI 7-16. American Society for Civil Engineers, Reston, VA. 2017.
- [10] Ganey R.: Seismic Design and Testing of Rocking Cross Laminated Timber Walls. M.S. Thesis, University of Washington, Seattle, WA. 2015.
- [11] Computers and Structures, Inc. CSI Analysis Reference Manual: For SAP2000, ETABS, SAFE, and CSI Bridge. Computers and Structures, Inc., Berkeley, CA. 2010.
- [12] The MathWorks, Inc. MATLAB, version 9.12.0.1884302 (R2022a). The MathWorks, Inc., Natick, MA. 2022.
- [13] Wilson A.: Numerical Modeling and Seismic Performance of Post-Tensioned Cross-Laminated Timber Rocking Walls. M.S. Thesis, Washington State University, Pullman, WA. 2018.
- [14] Pei, S., J. W. van de Lindt, A. R. Barbosa, J. W. Berman, E. McDonnell, J. D. Dolan, H.-E. Blomgren, R. B. Zimmerman, D. Huang, and S. Wichman: Experimental Seismic Response of a Resilient 2-Story Mass-Timber Building with Post-Tensioned Rocking Walls. *Journal of Structural Engineering*, 145 (11): 04019120, 2019.
- [15] Pacific Earthquake Engineering Research Center. PEER Ground Motion Database. 2013. <https://ngawest2.berkeley.edu/>. Accessed December 2019.
- [16] Applied Technology Council. Quantification of Building Seismic Performance Factors. Report No. P-695, FEMA. 2009.
- [17] Pei, S., J. W. van de Lindt, and M. Popovski: Approximate R-Factor for Cross-Laminated Timber Walls in Multistory Buildings. *Journal of Architectural Engineering*, 19 (4): 245–255, 2013.
- [18] Structurlam. CrossLam® CLT - Technical Design Guide - v4.0-USA. Structurlam, Penticton, BC. 2018.
- [19] Oregon State University and Portland State University. Framework Project. Deliverable 18: Structural Testing. Corvallis, OR, and Portland, OR. 2017.
- [20] Simpson Strong-Tie. F-L-SRS18 - Design Guide: Strong-Rod™ Systems. Simpson Strong-Tie Company Inc. 2018.